nature medicine

Antiretroviral dynamics determines HIV evolution and predicts therapy outcome

Daniel I S Rosenbloom[1,5], Alison L Hill[1,2,5], S Alireza Rabi[3,5], Robert F Siliciano[3,4] & Martin A Nowak[1]

Despite the high inhibition of viral replication achieved by current anti-HIV drugs, many patients fail treatment, often with emergence of drug-resistant virus. Clinical observations show that the relationship between adherence and likelihood of resistance differs dramatically among drug classes. We developed a mathematical model that explains these observations and predicts treatment outcomes. Our model incorporates drug properties, fitness differences between susceptible and resistant strains, mutations and adherence. We show that antiviral activity falls quickly for drugs with sharp dose-response curves and short half-lives, such as boosted protease inhibitors, limiting the time during which resistance can be selected for. We find that poor adherence to such drugs causes treatment failure via growth of susceptible virus, explaining puzzling clinical observations. Furthermore, our model predicts that certain single-pill combination therapies can prevent resistance regardless of patient adherence. Our approach represents a first step for simulating clinical trials of untested anti-HIV regimens and may help in the selection of new drug regimens for investigation.

The prognosis of HIV infection has dramatically improved since the introduction of highly active antiretroviral therapy (HAART), which, when successful, can bring viral loads below the detection limit, improve immune function and prevent progression to AIDS[1]. Although a complete understanding of how virologic, pharmacologic and host factors interact to determine therapeutic outcome is still lacking, it is clear that a major obstacle to successful treatment is suboptimal drug adherence. Nonadherence can lead to virologic failure and the emergence of drug resistance[2–5].

Because of their high antiviral activity, protease inhibitors are crucial in HIV-1 treatment and are used in three of the five recommended initial regimens and many salvage regimens[6]. Clinical trials have shown that for many drug combinations involving protease inhibitors, treatment failure occurs without resistance mutations in the viral gene encoding protease[7–10], though mutations conferring resistance to other drugs in the regimen are often found. It is generally believed that combination therapy works because it is unlikely that multiple mutations conferring resistance to all drugs in the combination will appear in the same viral genome. Thus, failure without protease inhibitor resistance is puzzling, because it seems to contradict this fundamental explanation for the success of HAART. It is commonly believed that protease inhibitors have a higher "barrier to resistance" than other drugs, meaning that clinically significant protease inhibitor resistance requires the accumulation of multiple mutations in the protease gene[11]. Protease inhibitor resistance also typically occurs at a narrower range of adherence levels than resistance to other drug classes[3,12]. Although these concepts are suggestive, no theory has been developed to explain why patients fail protease inhibitor–based regimens without protease inhibitor resistance.

A resistance mutation may exist before treatment in the latent or active viral populations or may arise during treatment[13]. Drug resistance develops clinically if the mutant strain is selected for over the wild-type strain. Selection depends on the fitness costs and benefits of the mutation, as well as on drug levels, which vary with the dosing interval, the drug half-life and the patient's adherence. Here we use a modeling approach to integrate these factors, enabling us to determine when a resistance mutation will be selected and to predict the outcome of therapy with different drugs. Our results explain the unique adherence-resistance relationship for protease inhibitors and show why patients fail protease inhibitor–based therapy without protease inhibitor resistance.

RESULTS

Defining the mutant selection window

Antiretroviral drugs reduce viral fitness in a dose-dependent manner (**Fig. 1a**). Viral fitness can be summarized as a single parameter, the basic reproductive ratio R_0, which encompasses all phases of the viral life-cycle[14] (**Supplementary Methods**). The Hill dose-response curve describes the relationship between drug concentration and R_0:

$$R_0(D) = \frac{R_{00}}{1 + \left(\frac{D}{\mathrm{IC}_{50}}\right)^m} \quad (1)$$

Here D is drug concentration, IC_{50} is the concentration at which 50% inhibition occurs, and m is a parameter determining steepness of the curve[15,16]. The numerator R_{00} is baseline fitness in the absence of treatment.

[1]Program for Evolutionary Dynamics, Department of Mathematics, Department of Organismic and Evolutionary Biology, Harvard University, Cambridge, Massachusetts, USA. [2]Biophysics Program and Harvard-MIT Division of Health Sciences and Technology, Harvard University, Cambridge, Massachusetts, USA. [3]Department of Medicine, Johns Hopkins University School of Medicine, Baltimore, Maryland, USA. [4]Howard Hughes Medical Institute, Baltimore, Maryland, USA. [5]These authors contributed equally to this work. Correspondence should be addressed to R.F.S. (rsiliciano@jhmi.edu) or M.A.N. (martin_nowak@harvard.edu).

Received 7 May; accepted 27 June; published online 2 September 2012; doi:10.1038/nm.2892

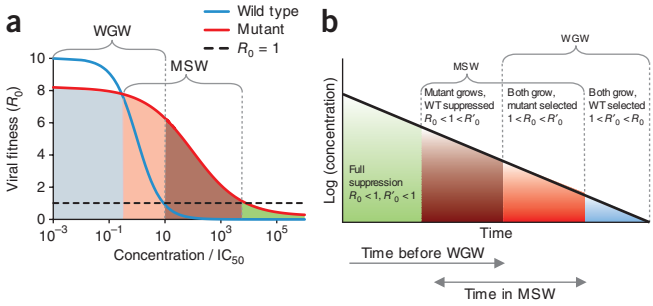

Figure 1 Drug concentrations determine the relative fitness of the wild-type virus and a resistant mutant. (**a**) The fitness of the wild-type virus (R_0, blue line) decreases with increasing drug concentration (here shown normalized by wild-type IC_{50}), following equation (1). A drug-resistant strain (R'_0, red line) is less fit than the wild type at low concentrations but more fit at higher concentrations, owing to an increased IC_{50} or a reduced slope. The MSW is the range of concentrations where a resistant mutant, if present, will grow faster than the wild type and still has $R'_0 > 1$. The WGW is the range of low concentrations where the wild type has $R_0 > 1$, leading to treatment failure without the need for resistance. For drug concentrations in the overlapping range of these windows, virologic failure can occur even without resistance but will be hastened by the appearance of a faster-growing mutant. (**b**) As drug concentrations decay after the last dose is taken, the viral fitness passes through four different selection ranges. Depending on the drug, dose level and mutation, not all of these ranges may exist. The time spent in each selection window is also determined by the drug half-life. WT, wild type.

A drug-resistant mutant is any viral variant that is less inhibited than the wild type for some drug concentration, described by the altered dose-response curve that determines R'_0, the basic reproductive ratio of the resistant virus:

$$R'_0(D) = \frac{R_{00}(1-s)}{1+\left(\frac{D}{\rho IC_{50}}\right)^{m(1+\sigma)}} \quad (2)$$

Mutations have a fitness cost, meaning that the drug-free fitness of the mutant virus is reduced by a fraction s ($0 < s < 1$). In the presence of the drug, the mutation confers a benefit, multiplying the IC_{50} by a factor ρ (the fold change in IC_{50}, $\rho > 1$). Many mutations also reduce the slope (m) of the dose-response curve by a fraction $\sigma < 0$ (ref. 17).

Virologic failure occurs when treatment fails to prevent the growth of virus to high levels. A viral strain grows when $R_0 > 1$. The strain with highest R_0 outcompetes others[14]. The range of drug concentrations where a resistant mutant can cause virologic failure is called the mutant selection window (MSW)[18,19]. Above the MSW, even replication of the mutant is suppressed ($R'_0(D) < 1$), although toxicity may prevent these drug concentrations from being achieved clinically. We here define the wild-type growth window (WGW), where drug concentrations are so low that wild-type virus is not adequately suppressed and failure can occur even without resistance ($R_0(D) > 1$).

The MSW explains therapy outcome patterns

To predict how well each drug suppresses growth of resistant and susceptible strains, we computed the time during a treatment interruption that a patient spends in the MSW and WGW. During treatment interruption, both R_0 and R'_0 increase. Up to four selection ranges can be identified (**Fig. 1b**). Using pharmacokinetic and pharmacodynamic data[16,17] (**Supplementary Table 1**), we determined the time spent in these ranges for 66 drug-mutation pairs (**Fig. 2a**) on the basis of their specific dose-response curves (**Fig. 2b–e**).

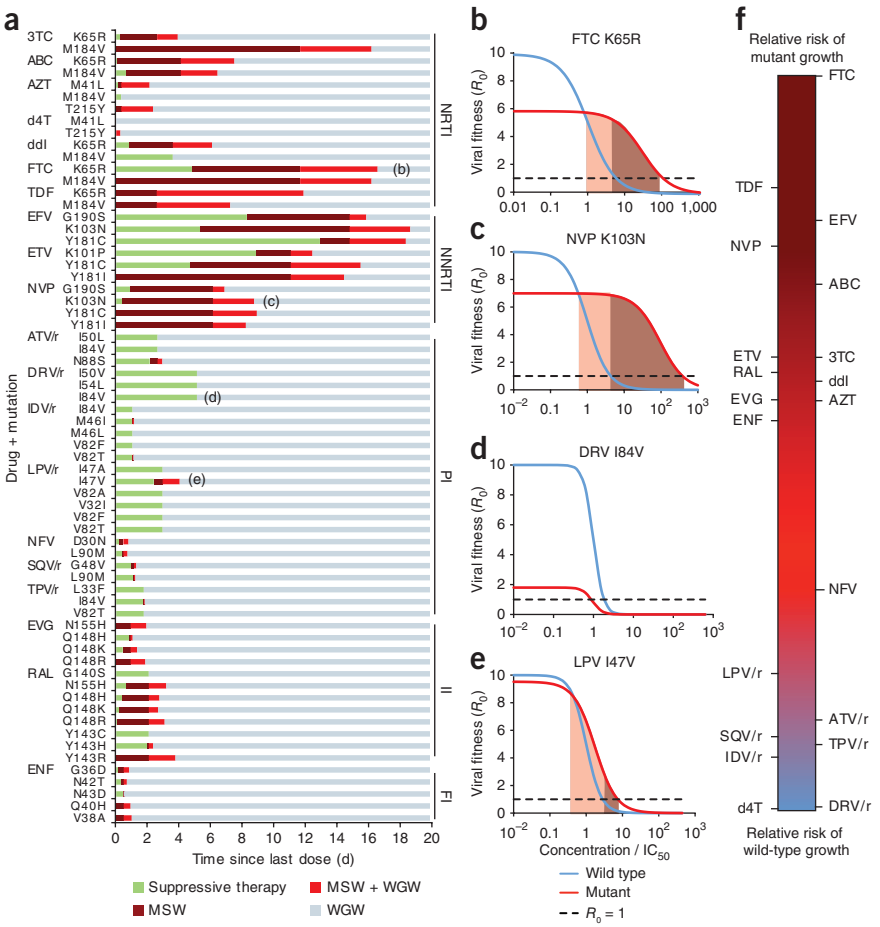

Figure 2 Selection windows can be calculated for particular drug-mutation pairs. (**a**) The distance to the right along each horizontal bar is the time since the last dose, and the color corresponds to the selection window during that time interval (described in **Fig. 1b**). (**b–e**) Examples of dose-response curves (showing drug concentration normalized by wild-type IC_{50}) for drug-mutation combinations indicated in **a**. Shading indicates the MSW. If the cost of a mutation is too high or its benefit (ρ or σ) too low, it is possible that the MSW does not exist. (**f**) Rank of each drug for relative risk of wild-type versus mutant virus growth, independent of the overall risk of therapy failure. For each drug, we show a 'synthetic', worst-case, single-nucleotide mutation (**Supplementary Methods** and **Supplementary Fig. 12**). PI, protease inhibitors; FI, fusion inhibitors; II, integrase inhibitors; ABC, abacavir; FTC, emtricitabine; ATV, atazanavir; TPV, tipranavir; EVG, elvitegravir. Protease inhibitors are often boosted (co-formulated) with ritonovir (/r), which interferes with breakdown in the liver and increases half-life.

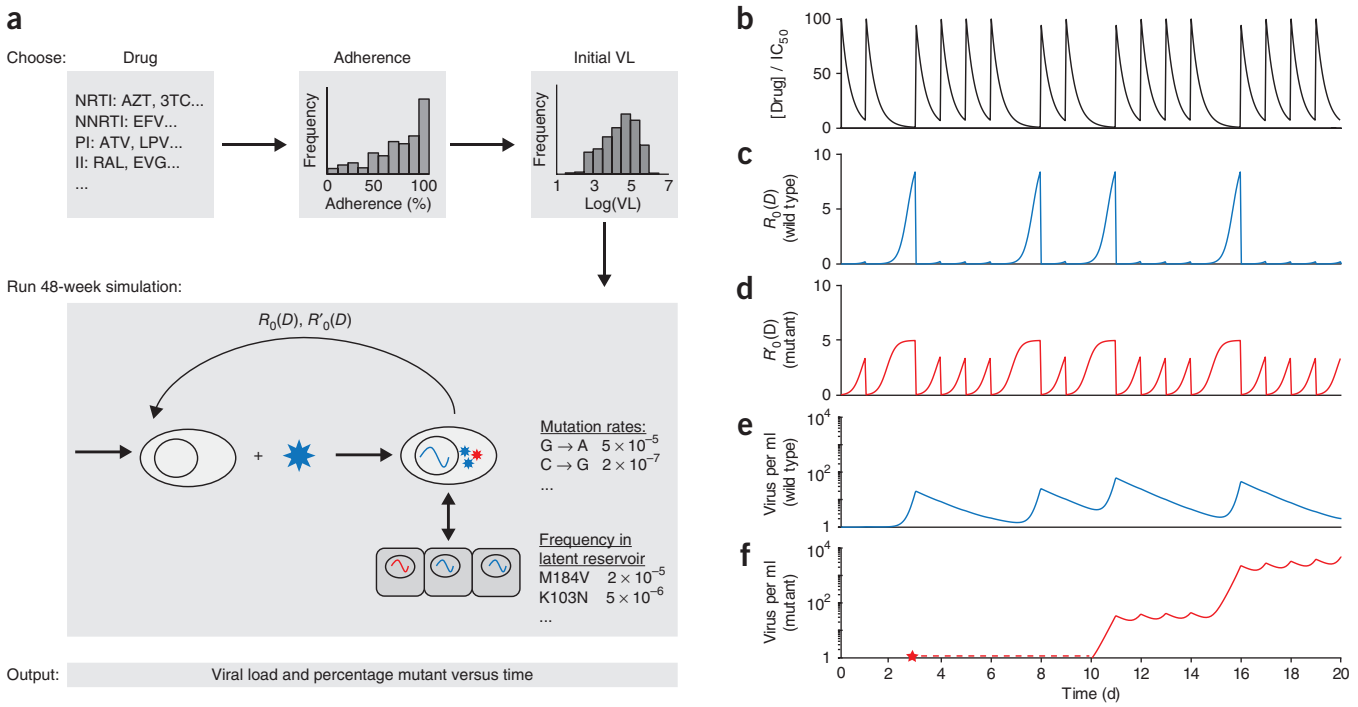

Figure 3 Schematic of algorithm for simulating viral dynamics in a patient undergoing treatment. (**a**) A single simulated patient takes a particular drug (or drug combination) with a designated adherence level, starting with an initial viral load (VL). Over a 48-week clinical trial, drug levels fluctuate and viral load levels are simulated according to a viral dynamics model. (**b**) Drug levels fluctuate according to patient's dosing pattern and pharmacokinetics (dose size, half-life, bioavailability); gaps show missed doses (figure shows single drug). (**c**) Wild-type viral fitness (R_0) fluctuates in response to drug concentration depending on the dose-response curve. (**d**) Fitness of drug-resistant strain (R'_0) depends on an altered dose-response curve; at high drug concentrations, mutant fitness exceeds that of the wild type. (**e**) Wild-type viral load depends on viral dynamics equations, which account for active replication, exit from the latent reservoir and competition between strains. (**f**) A mutant virus may appear (red star) but be below the threshold for detection (dotted red line) before eventually leading to virologic failure. Throughout the figure, blue coloring refers to wild-type virus and red coloring to mutant virus.

For each pair, we determined how soon after the most recent dose the mutant or wild-type virus starts to grow. This quantity is shorter than the expected time until virologic failure, which requires plasma HIV RNA to reach detectable levels and may also depend on the time until mutant virus appears. We examined here only single-point mutations that are fully characterized by their effect on the dose-response curve (equation (2), **Supplementary Tables 2** and **3**). For this reason, we caution that our results may be overly optimistic, as viruses with multiple resistance mutations often appear during infection. The use of our results for clinical recommendations is therefore premature. Extension of this model to multiple mutations is discussed below.

Successful treatment must both minimize the time spent in the MSW and delay entry into the WGW. These two goals are in tension, as shortening the time spent in the MSW (for example, by decreasing drug half-life) can also hasten entry into the WGW (**Fig. 1b**). Results from our model (**Fig. 2a**) suggest that non-nucleoside reverse-transcriptase inhibitors (NNRTIs) are protected against failure via wild-type virus due to their long half-lives but are vulnerable to mutation due to the time spent in the MSW. Protease inhibitors are at the opposite end of the spectrum, with little time spent in the MSW but rapid entry into the WGW. This behavior is caused by high slope parameters (extreme sensitivity to changes in concentration) and short half-lives. These results explain the unique trade-off presented by protease inhibitor therapy: greater protection against the evolution of resistance but vulnerability to wild-type–based virologic failure after short treatment interruptions. This feature is depicted schematically by plotting the drugs along a single axis, which measures the relative risk of mutant growth versus wild-type growth, independent of the overall risk of virologic failure (**Fig. 2f** and **Supplementary Methods**).

Simulation of clinical outcomes

Whereas the MSW and WGW concepts describe instantaneous growth of mutant and wild-type virus for a given drug concentration, virologic failure depends on sustained growth and, therefore, drug concentrations over time. To explain clinical observations across drug classes and adherence levels, we developed a stochastic model of viral evolution (**Fig. 3** and Methods). Our model builds on the large body of previous work modeling HIV therapy[14,20–23] by integrating new data on class-specific drug properties[16] and realistic costs and benefits of mutations[17]. We also modified past approaches by allowing drug concentrations, and hence R_0, to fluctuate, rather than taking time-averages.

We first simulated 48-week trials of single agents in a cohort of patients. The results are presented in two ways: as outcome versus patient adherence at the trial endpoint (**Fig. 4a**) and as outcome versus time for a distribution of patient adherence levels (**Fig. 4b**,**c**).

Consistent with a previous meta-analysis of combination therapy clinical trials[24], our model predicts that the level of adherence necessary for mutant virologic failure differs by drug class (**Fig. 5**). Specifically, for the NNRTIs efavirenz (EFV) and etravirine (ETV), the risk of mutant virologic failure is greatest at low adherence levels; for unboosted protease inhibitors, the risk peaks at a higher adherence level and remains substantial up to 100% adherence; for

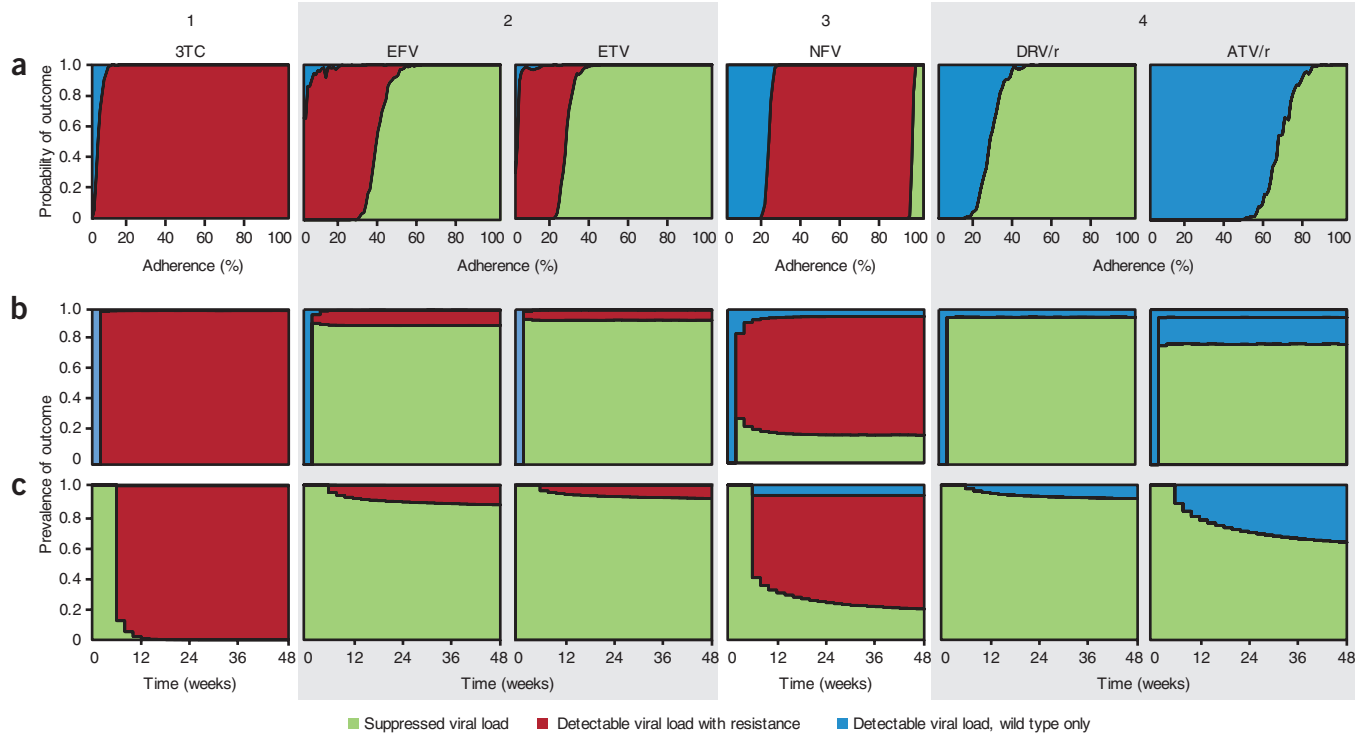

Figure 4 Outcomes for simulated patients in a clinical trial. (**a**–**c**) The height of the area shaded indicates probability of the corresponding outcome at a given adherence level (**a**) or time point (**b**,**c**). (**a**) Adherence is defined as the fraction of scheduled doses taken. These are maintenance trials (see Online Methods). (**b**,**c**) Measurements are taken every 2 weeks for simulated patients with a distribution of adherence levels (**Supplementary Methods** and **Supplementary Fig. 13b**). (**b**) Suppression trials (see Online Methods). (**c**) Maintenance trials. (1) 3TC therapy (pattern includes AZT, ABC, d4T, ENF, EVG, FTC, NVP, RAL, TDF). (2) EFV and ETV therapy. (3) NFV therapy (pattern includes ddI). (4) DRV/r and ATV/r therapy (pattern includes ATV, TPV/r; variation on this pattern described in the Results includes LPV/r, SQV, SQV/r IDV, IDV/r).

boosted protease inhibitors (paired with ritonavir to increase half-life), resistance occurs infrequently and at intermediate adherence levels. Researchers have previously argued that drug half-life and fitness costs of mutations are key factors explaining these general trends[3,12]. By incorporating these factors as parameters, our model formalizes this argument.

In examining simulations of each drug individually (**Supplementary Figs. 1**–**7**), we found four qualitative patterns of outcome, which correspond closely—but not exactly—to drug class (**Fig. 4**).

For most nucleoside reverse-transcriptase inhibitors (NRTIs), the integrase inhibitors, the fusion inhibitor enfuvirtide (ENF) and the NNRTI nevirapine (NVP), even perfect adherence led to mutant virologic failure in all simulated patients. As adherence declined, some wild-type virologic failure occurred. Virologic failure and resistance occurred soon after the trials started. These results are consistent with the notion that monotherapy often leads to rapid evolution of resistance.

For most protease inhibitors and the NNRTIs EFV and ETV, however, perfect adherence resulted in treatment success in simulations. Control of viral replication has been observed in a substantial fraction of patients in protease inhibitor monotherapy trials[25], but similar trials with EFV and ETV have not been carried out. In simulations, declining adherence affected performance of these two drug classes differently.

For the NNRTIs EFV and ETV, there was a large range of low-to-intermediate adherence for which mutant virologic failure was likely. Below this range, wild-type virologic failure became increasingly likely, whereas above this range therapy in the simulated patients succeeded. The size of this range is explained by the low fitness costs of

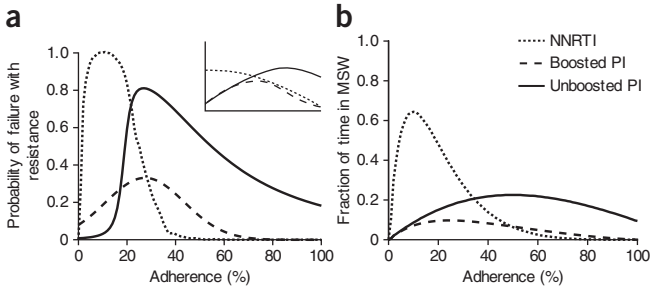

Figure 5 Our calculated adherence-resistance relations are in agreement with those observed in clinical trials. (**a**) Adherence versus simulated probability of resistance in a 48-week suppression trial for a protease inhibitor, a boosted protease inhibitor and an NNRTI. The inset shows a qualitative summary of results from a meta-analysis of clinical trials[24], which agrees with our simulations. (**b**) Adherence versus fraction of time spent in the MSW for the same drugs. Adherence-resistance trends demonstrate that time in MSW is a good proxy for the risk of mutant-based virologic failure. For both plots, curves were generated by averaging over all boosted protease inhibitors, all unboosted protease inhibitors, and the NNRTIs EFV and ETV. Protease inhibitor curves in **a** were fitted to skewed-T distributions to smooth step-like behavior. NVP, which was excluded from this figure, shows a different pattern from the other two NNRTIs; specifically, mutant virologic failure can occur even for perfect adherence (**Supplementary Figs. 1** and **2**).

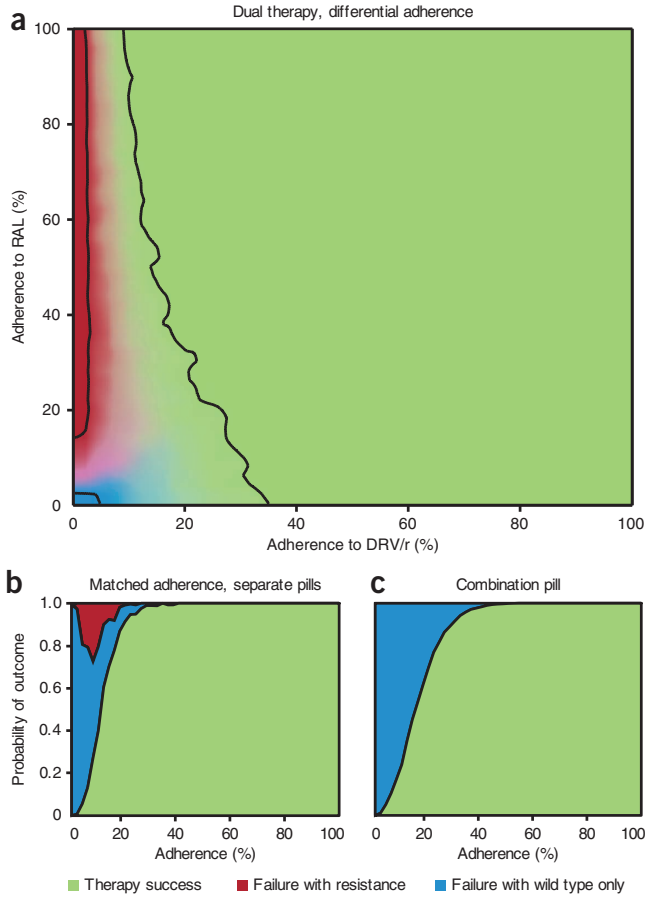

Figure 6 Outcomes of DRV/r plus RAL dual suppression therapy simulations, considering resistant mutants for both drugs. (**a**) Each drug is taken independently, and adherence may differ between them. The brightness of each color at a particular point indicates the probability of the corresponding outcome, with the black contours showing where each outcome occurs 95% of the time. Success depends largely on adherence to DRV/r (success is almost certain if adherence is >50%), whereas the type of failure is determined by adherence to RAL (resistance is almost certain if adherence is >30%). All failure via resistance is due to RAL mutant–based virologic failure. DRV mutant–based virologic failure (virologic failure) never occurs in the simulations. (**b**,**c**) Drugs are taken with equal average adherence. The height of the area shaded indicates probability of the corresponding outcome at that adherence level. (**b**) Drugs are taken as separate pills. Average adherence is the same, but pills are taken independently. (**c**) Drugs are packaged as a combination pill and are always taken together. Mutant virologic failure occurs only when the two drugs are given in separate pills; combination pills eliminate mutant virologic failure but increase the adherence required for near-certain success.

drug-resistant mutations and long half-lives of NNRTIs, which allowed the patient to remain within the MSW for a substantial duration (suggested in ref. 26).

The protease inhibitor nelfinavir (NFV) and the NRTI didanosine (ddI) showed a large range of intermediate adherence leading to mutant virologic failure. Near-perfect adherence was required for treatment success. Under most clinical settings (adherence <95%), our model predicts that these drugs perform similarly to monotherapy with other NRTIs, typically leading to mutant virologic failure.

For many protease inhibitors, a decline from perfect adherence led abruptly from success to wild-type virologic failure, with little or no intermediate range for mutant virologic failure. This result explains the outcomes of clinical studies, which have shown that virologic failure in many boosted protease inhibitor–based regimens (including monotherapy) does not require the evolution of resistance[7–9]. Variations on this pattern exist for some protease inhibitors: simulations of lopinavir (LPV/r), saquinavir (SQV, SQV/r), and indinavir (IDV, IDV/r) showed mutant virologic failure at low and moderate adherence levels, mainly for trials where the initial viral load was high. Still, like all the protease inhibitors simulated except NFV, as adherence declined from the successful range, the first failing outcome observed was wild-type virologic failure (**Supplementary Figs. 1** and **2**).

We also examined the sensitivity of our results to changes in the baseline viral fitness, R_{00} (**Supplementary Figs. 8** and **9**). As the intracellular half-lives of several NRTIs are not definitively established, we tested a range of half-lives for lamivudine (3TC), azidothymidine (AZT), stavudine (d4T), ddI and tenofovir disoproxil fumarate (TDF) (**Supplementary Fig. 10**). Against a strain with higher R_{00}, higher adherence levels were required for treatment success, and there was a wider range of adherence levels for which mutant virologic failure occurred. The effect of increasing half-life was drug dependent, but for most NRTIs simulated, it increased the likelihood of mutant virologic failure.

Explaining outcomes of combination therapy

Equipped with a model of drug interaction, we were able to extend the simulations to combination therapy (**Supplementary Methods** and **Supplementary Fig. 11**). For proof of concept, we use a two-drug combination of the boosted protease inhibitor darunavir (DRV/r) with the integrase inhibitor raltegravir (RAL). The combined effect of these two drugs is given by a Bliss-independent[27] interaction pattern[28], which describes drugs acting on different targets, therefore reducing viral replication multiplicatively. In a recent DRV/r-RAL clinical trial[8], patients experiencing virologic failure had their plasma viral population genotyped. Although 17% of patients tested positive for RAL-resistance mutations in the gene encoding integrase, no patients tested positive for DRV resistance in the gene encoding protease[8]. Our simulation is consistent with this study: treatment failure occurred without DRV resistance (**Fig. 6a**).

RAL-resistant mutants were selected for only when the concentration of DRV/r was low and the concentration of RAL was moderate to high (**Supplementary Fig. 11**). This state of "effective monotherapy"[26] can occur if the drugs are administered as separate pills. If, however, dual therapy were administered as a combination pill, then the two concentrations would rise and fall roughly together, reducing the chance that they reach the discordant levels that select for resistance. Simulation of dual therapy as a single combination pill verified this hypothesis. However, this protection from resistance came at a cost: higher adherence was required to prevent wild-type virologic failure. For example, to ensure a 95% chance of success in the simulation, a patient taking separate pills must be 25% adherent to each pill (**Fig. 6b**), but 35% adherent to a combination pill (**Fig. 6c**). We expect this trend to apply to other drug combinations.

DISCUSSION

Recent efforts to quantify pharmacodynamics[16,17,29], combined with insights into patients' drug-taking behavior[30], have enabled us to develop what is to our knowledge the first explanatory model of virologic failure in agreement with clinical trials. All parameters in our model have direct physical interpretations, and their values were taken directly, or derived from, previous literature. The model was not

fit or trained to match clinical data. Despite our model's simplicity, it can explain the clinically observed drug-class–specific relationship between adherence and outcome[24] (**Fig. 5**). Even without full viral dynamic simulations, a straightforward analysis of the mutant selection window can explain why certain drugs are more likely to select for resistance (**Figs. 2f** and **5b**).

In addition, we address a long-standing mystery of antiretroviral therapy. Even when failure of protease inhibitor–based regimens is documented, mutations that confer resistance to the protease inhibitor appear infrequently[7–10]. Although it is possible that mutations may occur outside the protease-encoding gene[31–34] and escape routine detection, our model provides a more straightforward explanation: due to the sharp slope of protease inhibitor dose-response curves[16], even relatively strong protease inhibitor resistance mutations are selected only in a narrow range of drug concentrations. Moreover, as protease inhibitor concentrations decay rapidly compared to other drugs, they traverse this narrow range quickly, leaving little time for a resistant strain to grow before wild-type–based virologic failure. We predict that patients who fail protease inhibitor therapy with wild-type virus should be able to re-suppress the virus if the same drug is taken with improved adherence. A previous study[12] observed this outcome in patients who failed LPV/r without detectable resistance. Even with protease inhibitors that are more susceptible to resistance, only wild-type virus is detectable when adherence dips below the level guaranteeing success, providing an antiresistance 'buffer' that may warn clinicians of resistance risk. NFV is the sole exception to this pattern, owing to its having the lowest slope and second-highest IC_{50} of the protease inhibitors and consistent with its documented vulnerability to resistance[12].

The tradeoff between protection from resistant and susceptible strains occurs not only between drug classes but also between different formulations of the same drugs. We predict that a new combination pill containing DRV/r and RAL would not lead to resistance, even though the current separate-pill formulation does. This result suggests that some combination pills may be 'resistance proof', but their known benefit of increasing patient adherence must be weighed against the fact that they require higher adherence to prevent wild-type–based virologic failure. This trade-off results from the possibility that a patient who is prescribed multiple pills may at times take only some of them[35], providing partial protection from the virus but allowing entry into a 'zone of monotherapy'[26] that can select for resistance.

We can extend our model to a broader range of combination therapies once interactions between drugs[28] are characterized; these interactions affect the evolution of resistance[36]. Our monotherapy results are a first step for examining how pharmacokinetics and pharmacodynamics determine treatment outcomes. These results can inform innovations in lower-cost maintenance therapy among highly adherent patients, for whom monotherapy shows promise but also poses resistance risks[25]. Specifically, on the basis of our simulations, we propose that EFV and ETV monotherapy may be promising avenues for further study, despite the disheartening performance of monotherapy with the first approved NNRTI, NVP[37], and the ambiguous performance of ETV-based HAART for patients with resistance to the NRTI backbone[38].

Simulations that start with a high viral load (suppression phase) and simulations that start with an undetectable viral load (maintenance phase) generally showed similar outcomes; however, for several drugs, failure with resistance was more likely during the suppression phase. Such differences are often attributed to the presence of preexisting mutants when viral load is high[39–42]. However, in our model, frequent reactivation from the latent reservoir provides a sufficient source of mutants during both phases (**Supplementary Tables 4** and **5**), and ongoing replication is an additional common cause of resistance (**Supplementary Figs. 6** and **7**). The key difference between the two phases is in how virologic failure is defined. As patients remained in suppression simulations until the predefined endpoint, wild-type growth sometimes preceded (and contributed to) growth of the mutant. More frequent measurement of viral load in maintenance simulations improved the chance that virologic failure was diagnosed before resistance reached detectable levels, consistent with clinical meta-analysis[43]. Also consistent with clinical observations[44], continuation of maintenance trials after rebound allowed the possibility of re-suppression, but it sometimes led to emergence of resistance (**Supplementary Fig. 5**).

It is difficult to quantitatively compare our simulations to clinical trials, as adherence is rarely precisely known. We suspect that our results are biased toward success for several reasons. First, we considered only single-point mutations, but strains with multiple mutations may lead to failure at higher adherence levels. Second, we considered neither correlations between consecutive missed doses nor variations in the time of day when a dose is taken, both factors that lead to longer treatment interruptions and increase the chance of virologic failure[20,45–48]. Third, as is common in models of viral dynamics, we assumed that the virus population is homogeneous and well mixed. Actual infections may include subpopulations that grow faster (higher R_0, for example, owing to cell-to-cell transmission[49]) or that reside in tissues that drugs do not fully penetrate[50–52]. For example, the concentration of EFV in the cerebrospinal fluid is only 0.5% of plasma concentrations[53]. As our predictions rely on plasma drug concentrations, they may be optimistic in the case of EFV (see ref. 54 for further discussion). In the absence of strong evidence for these effects, suboptimal adherence is the most likely cause of treatment failure. Given the above limitations, our modeling results should not be taken as clinical recommendations at this stage.

Patients experiencing virologic failure may not respond to a similar regimen in the future[45,55,56], but the precise reasons for this are not clear. The simplest explanation is that growth of a resistant strain during prior treatment makes it more likely this strain will exist in the future[57]. This explanation assumes that, in the absence of prior growth, most resistant mutants are relatively rare. If the diversity (effective population size) of the latent reservoir is not severely depleted over time, then our calculations contradict this assumption for single mutations: even in the absence of prior treatment, a majority of mutations exit the reservoir every few weeks. Resistance is then available to be selected regardless of prior growth. The occurrence of multiple mutations within the same viral genome is unlikely, however, without prior growth. To explain generally how prior virologic failure undermines future treatment, we need to model the long-term accumulation of multistep mutations in the viral population[58,59]. To build such models, it will be important to understand interactions between mutations (including compensatory mutations[54]) and account for recombination[60].

We have emphasized here the variable nature of anti-HIV drug resistance. Common practice classifies a genotype as resistant if it is associated with virologic failure in a meta-analysis of clinical outcomes; otherwise it is sensitive. This categorization is misleading: a mutation's ability to promote viral growth depends on all of the drugs in a regimen, adherence and the other mutations present. As standards of care evolve and study populations change, a mutation may gain or lose resistant status as a result of shifts in these confounding variables.

Our model provides a rigorous alternative for evaluating resistance, by using mechanistic parameters to predict clinical outcomes. Our framework can help researchers prioritize drugs for clinical trials and select regimens for personalized HIV treatment.

METHODS

Methods and any associated references are available in the online version of the paper.

Note: Supplementary information is available in the online version of the paper.

ACKNOWLEDGMENTS

We thank T. Antal, I. Božić, F. Fu, M. Sampah and L. Shen for discussion during the conception of this work, and we thank J. Gallant, J.-B. Michel and P. Pennings for their comments on the manuscript. We thank D. Bangsberg of Massachusetts General Hospital for supplying adherence data from the REACH study (supported by US National Institutes of Health grant R01 MH054907). Simulations were run on the Odyssey cluster supported by the Research Computing Group of Harvard University. We are grateful for support from the US National Institutes of Health (R01 AI081600 (R.F.S., S.A.R.), R01 GM078986 (M.A.N., A.L.H.)), the Bill & Melinda Gates Foundation (M.A.N., A.L.H.), a Cancer Research Institute Fellowship (S.A.R.), a US National Science Foundation Graduate Research Fellowship (D.I.S.R.), the Howard Hughes Medical Institute (R.F.S., S.A.R.), a Canadian Natural Sciences and Engineering Research Council Post-Graduate Scholarship (A.L.H.), the John Templeton Foundation (M.A.N.) and J. Epstein (M.A.N.).

AUTHOR CONTRIBUTIONS

D.I.S.R., A.L.H. and S.A.R. designed the models and conducted the simulations. D.I.S.R., A.L.H., S.A.R., R.F.S. and M.A.N. conceived of the study and wrote the manuscript.

COMPETING FINANCIAL INTERESTS

The authors declare no competing financial interests.

Published online at http://www.nature.com/doifinder/10.1038/nm.2892.
Reprints and permissions information is available online at http://www.nature.com/reprints/index.html.

1. Palella, F.J. *et al.* Declining morbidity and mortality among patients with advanced human immunodeficiency virus infection. HIV Outpatient Study Investigators. *N. Engl. J. Med.* **338**, 853–860 (1998).
2. Vanhove, G.F., Schapiro, J.M., Winters, M.A., Merigan, T.C. & Blaschke, T.F. Patient compliance and drug failure in protease inhibitor monotherapy. *J. Am. Med. Assoc.* **276**, 1955–1956 (1996).
3. Gardner, E.M., Burman, W.J., Steiner, J.F., Anderson, P.L. & Bangsberg, D.R. Antiretroviral medication adherence and the development of class-specific antiretroviral resistance. *AIDS* **23**, 1035–1046 (2009).
4. Maggiolo, F. *et al.* Effect of adherence to HAART on virologic outcome and on the selection of resistance-conferring mutations in NNRTI- or PI-treated patients. *HIV Clin. Trials* **8**, 282–292 (2007).
5. Harrigan, P.R. *et al.* Predictors of HIV drug-resistance mutations in a large antiretroviral- naive cohort initiating triple antiretroviral therapy. *J. Infect. Dis.* **191**, 339–347 (2005).
6. US Department of Health and Human Services Panel on Antiretroviral Guidelines for Adults & Adolescents. Guidelines for the use of antiretroviral agents in HIV-1-infected adults and adolescents. <http://aidsinfo.nih.gov/contentfiles/AdultandAdolescentGL.pdf> (2011).
7. Arribas, J.R. *et al.* The MONET trial: darunavir/ritonavir with or without nucleoside analogues, for patients with HIV RNA below 50 copies/ml. *AIDS* **24**, 223–230 (2010).
8. Taiwo, B. *et al.* Efficacy of a nucleoside-sparing regimen of darunavir/ritonavir plus raltegravir in treatment-naive HIV-1-infected patients (ACTG a5262). *AIDS* **25**, 2113–2122 (2011).
9. Havlir, D.V. *et al.* Drug susceptibility in HIV infection after viral rebound in patients receiving indinavir-containing regimens. *J. Am. Med. Assoc.* **283**, 229–234 (2000).
10. Pulido, F., Arribas, J., Hill, A. & Moecklinghoff, C. No evidence for evolution of genotypic resistance after three years of treatment with darunavir/ritonavir, with or without nucleoside analogues. *AIDS Res. Hum. Retroviruses* published online, doi:10.1089/aid.2011.0256 (20 April 2012).
11. Condra, J.H. Resistance to HIV protease inhibitors. *Haemophilia* **4**, 610–615 (1998).
12. Kempf, D.J. *et al.* Incidence of resistance in a double-blind study comparing lopinavir/ritonavir plus stavudine and lamivudine to nelfinavir plus stavudine and lamivudine. *J. Infect. Dis.* **189**, 51–60 (2004).
13. Noë, A., Plum, J. & Verhofstede, C. The latent HIV-1 reservoir in patients undergoing HAART: an archive of pre-HAART drug resistance. *J. Antimicrob. Chemother.* **55**, 410–412 (2005).
14. Nowak, M.A. & May, R.M.C. *Virus Dynamics: Mathematical Principles of Immunology and Virology* (Oxford University Press, USA, 2000).
15. Chou, T.-C. Derivation and properties of Michaelis-Menten type and Hill type equations for reference ligands. *J. Theor. Biol.* **59**, 253–276 (1976).
16. Shen, L. *et al.* Dose-response curve slope sets class-specific limits on inhibitory potential of anti-HIV drugs. *Nat. Med.* **14**, 762–766 (2008).
17. Sampah, M.E.S., Shen, L., Jilek, B.L. & Siliciano, R.F. Dose-response curve slope is a missing dimension in the analysis of HIV-1 drug resistance. *Proc. Natl. Acad. Sci. USA* **108**, 7613–7618 (2011).
18. Drlica, K. The mutant selection window and antimicrobial resistance. *J. Antimicrob. Chemother.* **52**, 11–17 (2003).
19. Drlica, K. & Zhao, X. Mutant selection window hypothesis updated. *Clin. Infect. Dis.* **44**, 681–688 (2007).
20. Wahl, L.M. & Nowak, M.A. Adherence and drug resistance: predictions for therapy outcome. *Proc. Bio. Sci.* **267**, 835–843 (2000).
21. Wu, H. *et al.* Modeling long-term HIV dynamics and antiretroviral response: effects of drug potency, pharmacokinetics, adherence, and drug resistance. *J. Acquir. Immune Defic. Syndr.* **39**, 272–283 (2005).
22. Smith, R.J. Adherence to antiretroviral HIV drugs: how many doses can you miss before resistance emerges? *Proc. Biol. Sci.* **273**, 617–624 (2006).
23. Rong, L., Feng, Z. & Perelson, A.S. Emergence of HIV-1 drug resistance during antiretroviral treatment. *Bull. Math. Biol.* **69**, 2027–2060 (2007).
24. Bangsberg, D.R., Moss, A.R. & Deeks, S.G. Paradoxes of adherence and drug resistance to HIV antiretroviral therapy. *J. Antimicrob. Chemother.* **53**, 696–699 (2004).
25. Pérez-Valero, I. & Arribas, J.R. Protease inhibitor monotherapy. *Curr. Opin. Infect. Dis.* **24**, 7–11 (2011).
26. Bangsberg, D.R., Kroetz, D.L. & Deeks, S.G. Adherence-resistance relationships to combination HIV antiretroviral therapy. *Curr. HIV/AIDS Rep.* **4**, 65–72 (2007).
27. Bliss, C.I. The toxicity of poisons applied jointly. *Ann. Appl. Biol.* **26**, 585–615 (1939).
28. Jilek, B.L. *et al.* A quantitative basis for antiretroviral therapy for HIV-1 infection. *Nat. Med.* **18**, 446–451 (2012).
29. Shen, L. *et al.* A critical subset model provides a conceptual basis for the high antiviral activity of major HIV drugs. *Sci. Transl. Med.* **3**, 91ra63 (2011).
30. Bangsberg, D.R. *et al.* Adherence-resistance relationships for protease and non-nucleoside reverse transcriptase inhibitors explained by virological fitness. *AIDS* **20**, 223–231 (2006).
31. Nijhuis, M. *et al.* A novel substrate-based HIV-1 protease inhibitor drug resistance mechanism. *PLoS Med.* **4**, e36 (2007).
32. Parry, C.M. *et al.* Gag determinants of fitness and drug susceptibility in protease inhibitor–resistant human immunodeficiency virus type 1. *J. Virol.* **83**, 9094–9101 (2009).
33. Dam, E. *et al.* Gag mutations strongly contribute to HIV-1 resistance to protease inhibitors in highly drug-experienced patients besides compensating for fitness loss. *PLoS Pathog.* **5**, e1000345 (2009).
34. Gupta, R.K. *et al.* Full length HIV-1 gag determines protease inhibitor susceptibility within *in vitro* assays. *AIDS* **24**, 1651–1655 (2010).
35. Gardner, E.M. *et al.* Differential adherence to combination antiretroviral therapy is associated with virological failure with resistance. *AIDS* **22**, 75–82 (2008).
36. Michel, J.-B., Yeh, P.J., Chait, R., Moellering, R.C. & Kishony, R. Drug interactions modulate the potential for evolution of resistance. *Proc. Natl. Acad. Sci. USA* **105**, 14918–14923 (2008).
37. Cheeseman, S.H. *et al.* Phase I/II evaluation of nevirapine alone and in combination with zidovudine for infection with human immunodeficiency virus. *J. Acquir. Immune Defic. Syndr. Hum. Retrovirol.* **8**, 141–151 (1995).
38. Ruxrungtham, K. *et al.* Impact of reverse transcriptase resistance on the efficacy of TMC125 (etravirine) with two nucleoside reverse transcriptase inhibitors in protease inhibitor-naive, nonnucleoside reverse transcriptase inhibitor-experienced patients: study TMC125–C227. *HIV Med.* **9**, 883–896 (2008).
39. Bonhoeffer, S. & Nowak, M.A. Pre-existence and emergence of drug resistance in HIV-1 infection. *Proc. Biol. Sci.* **264**, 631–637 (1997).
40. Paredes, R. *et al.* Pre-existing minority drug-resistant HIV-1 variants, adherence, and risk of antiretroviral treatment failure. *J. Infect. Dis.* **201**, 662–671 (2010).
41. Jourdain, G. *et al.* Association between detection of HIV-1 DNA resistance mutations by a sensitive assay at initiation of antiretroviral therapy and virologic failure. *Clin. Infect. Dis.* **50**, 1397–1404 (2010).
42. Simen, B.B. *et al.* Low-abundance drug-resistant viral variants in chronically HIV-infected, antiretroviral treatment–naive patients significantly impact treatment outcomes. *J. Infect. Dis.* **199**, 693–701 (2009).
43. Gupta, R.K. *et al.* Virological monitoring and resistance to first-line highly active antiretroviral therapy in adults infected with HIV-1 treated under who guidelines: a systematic review and meta-analysis. *Lancet Infect. Dis.* **9**, 409–417 (2009).
44. Hoffmann, C.J. *et al.* Viremia, resuppression, and time to resistance in human immunodeficiency virus (HIV) subtype c during first-line antiretroviral therapy in South Africa. *Clin. Infect. Dis.* **49**, 1928–1935 (2009).
45. Parienti, J.-J. Not all missed doses are the same: sustained NNRTI treatment interruptions predict HIV rebound at low-to-moderate adherence levels. *PLoS ONE* **3**, e2783 (2008).

46. Parienti, J.-J. Average adherence to boosted protease inhibitor therapy, rather than the pattern of missed doses, as a predictor of HIV RNA replication. *Clin. Infect. Dis.* **50**, 1192–1197 (2010).
47. Liu, H. *et al.* Repeated measures analyses of dose timing of antiretroviral medication and its relationship to HIV virologic outcomes. *Stat. Med.* **26**, 991–1007 (2007).
48. Kastrissios, H. *et al.* Characterizing patterns of drug-taking behavior with a multiple drug regimen in an AIDS clinical trial. *AIDS* **12**, 2295–2303 (1998).
49. Sigal, A. *et al.* Cell-to-cell spread of HIV permits ongoing replication despite antiretroviral therapy. *Nature* **477**, 95–98 (2011).
50. Kepler, T.B. & Perelson, A.S. Drug concentration heterogeneity facilitates the evolution of drug resistance. *Proc. Natl. Acad. Sci. USA* **95**, 11514–11519 (1998).
51. Schnell, G., Price, R.W., Swanstrom, R. & Spudich, S. Compartmentalization and clonal amplification of HIV-1 variants in the cerebrospinal fluid during primary infection. *J. Virol.* **84**, 2395–2407 (2010).
52. van Marle, G. *et al.* Compartmentalization of the gut viral reservoir in HIV-1 infected patients. *Retrovirology* **4**, 87 (2007).
53. Best, B.M. *et al.* Efavirenz concentrations in CSF exceed IC_{50} for wild-type HIV. *J. Antimicrob. Chemother.* **66**, 354–357 (2011).
54. Hill, A.L., Rosenbloom, D.I.S. & Nowak, M.A. Evolutionary dynamics of HIV at multiple spatial and temporal scales. *J. Mol. Med.* **90**, 543–561 (2012).
55. Hirsch, M.S. *et al.* Antiretroviral drug resistance testing in adult HIV-1 infection: recommendations of an International AIDS Society–USA panel. *J. Am. Med. Assoc.* **283**, 2417–2426 (2000).
56. Lima, V.D. *et al.* Differential impact of adherence on long-term treatment response among naive HIV-infected individuals. *AIDS* **22**, 2371–2380 (2008).
57. Boltz, V.F. *et al.* Role of low-frequency HIV-1 variants in failure of nevirapine-containing antiviral therapy in women previously exposed to single-dose nevirapine. *Proc. Natl. Acad. Sci. USA* **108**, 9202–9207 (2011).
58. Nowak, M.A. *et al.* Antigenic diversity thresholds and the development of AIDS. *Science* **254**, 963–969 (1991).
59. Shankarappa, R. *et al.* Consistent viral evolutionary changes associated with the progression of human immunodeficiency virus type 1 infection. *J. Virol.* **73**, 10489–10502 (1999).
60. Neher, R.A. & Leitner, T. Recombination rate and selection strength in HIV intra-patient evolution. *PLoS Comput. Biol.* **6**, e1000660 (2010).

ONLINE METHODS

Pharmacokinetics, pharmacodynamics and the mutant selection window. Viral fitness followed equation (1) with parameters R_{00}, IC_{50} and m. Fitness of resistant mutants followed equation (2) with parameters s, ρ and σ. (**Supplementary Tables 1–3**). Relative wild-type and mutant viral fitness values $R_0(D) / R_{00}$ and $R'_0(D) / R_{00}$ were measured using *in vitro* assays and were fit to Hill curves to determine the parameters IC_{50}, m, σ, ρ and s; these values were reported previously[16,17]. We estimated absolute *in vivo* viral fitness in the absence of drugs (R_{00}) using measurements from previous studies (**Supplementary Methods**). We modeled drug concentration as instantaneously increasing after a dose to the steady-state peak concentration (C_{max}) and then decaying exponentially (with half-life $T_{1/2}$) to the trough concentration (C_{min}) before the subsequent dose. When doses were missed (representing suboptimal adherence), the concentration continued to decay, and a subsequent dose increased the concentration by $\Delta C = C_{max} - C_{min}$.

We determined the bounds of the MSW by solving for D in $R_0(D) = R'_0(D)$ and $R'_0(D) = 1$. We determined the upper bound of the WGW by solving $R_0(D) = 1$. We computed the time after a single dose when a particular concentration D was reached by solving for t in $D = C_{max} \times 2^{-t/T_{1/2}}$.

The MSW concept as applied here to antiretroviral therapy was adapted from the extensive literature on antibiotic resistance. Both *in vitro* and *in vivo*, drug concentrations that fluctuate within the MSW lead to the development of resistance, but those outside it do not (reviewed in ref. 19). Although some studies of antibiotic-resistant *Escherichia coli* have found no upper limit to the MSW[61], no such results are known for antiretroviral resistance. The definition of the MSW most commonly used in antibiotic work is slightly different from the one we use, with the lower limit defined as $R_0(D) = 1$ because of experimental constraints[18]. We have chosen to modify this definition, as selection for the mutant can occur even at lower drug concentrations where $R_0(D) > 1$ (ref. 62). The MSW and WGW can be described for each drug during combination therapy (**Supplementary Methods**).

Simulation of the viral dynamics model. Our model for HIV dynamics during antiretroviral drug treatment uses equations common in the literature[14]. These equations track the number of uninfected $CD4^+$ cells, amount of free virus and number of infected $CD4^+$ cells. A constant number of uninfected cells are produced each day, and they die at a constant rate. Cells are infected at a rate proportional to the number of uninfected cells, the amount of virus, and the viral fitness. Virion production from infected cells is described by the burst rate, and virions are cleared at a constant rate. Infected cells have a higher death rate than uninfected cells. Additionally, we include a population of long-lived infected cells in the latent reservoir, which activate at a constant daily rate regardless of viral fitness. Because we are interested only in viral dynamics during treatment and at the initial stages of failure, we have ignored the effects of the immune response. Viral fitness, and hence the rate of infection of new $CD4^+$ cells, is determined by the baseline R_0 and the drug concentration. All equations and parameters are given in the **Supplementary Methods** and **Supplementary Table 6**. In the **Supplementary Methods**, we also derive a simplified form of HIV dynamics that requires fewer parameters and only one state variable per viral strain; we used this simplified model to design our simulations. More detailed models that explicitly track multiple stages of the viral life cycle may more accurately reflect some short-term dynamics, such as lags in viral growth during acute infection or lags in viral decay during the early days of treatment[63,64]. Summarizing viral fitness by a single parameter (R_0) smoothes out these dynamics.

There may be multiple strains of virus (wild-type and mutants) and consequently multiple types of infected cells. Even in the absence of drug, mutations will arise due to random errors in replication, though they will be selected against due to their fitness cost (s). Each mutation appears at a rate u that depends on the particular nucleotide changes required to effect the desired amino acid substitution (**Supplementary Tables 2**, **3** and **7**). The balance between these two processes results in all mutations being present in the population at an expected low level u / s, called mutation-selection equilibrium[14,65]. We assume that the plasma virus population reaches this equilibrium in each patient before treatment (that is, that sufficient time has passed between initial infection and treatment initiation and that no prior treatment has selected for resistance to the particular drug being studied) and that the population in the latent reservoir is representative of the plasma population (**Supplementary Tables 4** and **5**). *De novo* mutations occur with a probability u during replication.

We used stochastic simulations to study the dynamics of the system described. Many mutations have been characterized for each drug, and to model a realistic worst-case scenario we considered a single synthetic mutant defined as having the highest benefits (ρ, negative σ), lowest cost (s), highest mutation rate and highest equilibrium frequency (due to mutation-selection balance) of all the single-nucleotide mutants known for that drug. Each monotherapy simulation therefore tracked only two strains, wild-type and mutant. For dual therapy, we considered three strains: wild-type, resistant to drug 1, and resistant to drug 2. Simulations modeled 48-week trials, using discrete time-steps of Δt = 30 min. All simulations were done in Matlab R2010b. The full details of the algorithm for simulating a single patient are given in the **Supplementary Methods**.

In maintenance trials, patients began with full viral suppression (2 RNA copies per ml, c ml^{-1}) and underwent monotherapy for 48 weeks or until virologic failure, whichever occurred first. Virologic failure was defined as 'confirmed rebound': two consecutive weekly measurements (starting at week 5) with viral load above 200 c ml^{-1}. In suppression trials, patients began with a realistic distribution of treatment-naive viral loads (between 3,000 and 10^6 c ml^{-1}) (**Supplementary Fig. 13a**) and underwent monotherapy for a full 48 weeks. We tracked measurements every 2 weeks. Virologic failure was defined as a viral load above 50 c ml^{-1} at week 48. In both types of trials, virologic failure was classified as 'with resistance' if at least 20% of the viral population at the time of detection was mutant.

We simulated imperfect adherence by allowing each dose to be missed with a constant probability given by the expected adherence level parameter. In reporting outcomes versus time, we simulated patients with a distribution of adherence levels taken from a study using unannounced pill counts[30]. For simulations with two drugs, the value of adherence may be different for each drug, allowing for 'differential adherence', which has been observed in many studies[35]. Even when adherence to the two drugs has the same average value, the drugs can be simulated as two separate pills (allowing each pill to be taken or forgotten independently) or as a single combination pill (causing the two drug concentrations to rise and fall in lockstep).

61. Zhao, X. & Drlica, K. Restricting the selection of antibiotic-resistant mutant bacteria: measurement and potential use of the mutant selection window. *J. Infect. Dis.* **185**, 561–565 (2002).
62. Gullberg, E. *et al.* Selection of resistant bacteria at very low antibiotic concentrations. *PLoS Pathog.* **7**, e1002158 (2011).
63. Sedaghat, A.R., Dinoso, J.B., Shen, L., Wilke, C.O. & Siliciano, R.F. Decay dynamics of HIV-1 depend on the inhibited stages of the viral life cycle. *Proc. Natl. Acad. Sci. USA* **105**, 4832–4837 (2008).
64. Ribeiro, R.M. *et al.* Estimation of the initial viral growth rate and basic reproductive number during acute HIV-1 infection. *J. Virol.* **84**, 6096–6102 (2010).
65. Ribeiro, R.M., Bonhoeffer, S. & Nowak, M.A. The frequency of resistant mutant virus before antiviral therapy. *AIDS* **12**, 461–465 (1998).

doi:10.1038/nm.2892